J. Earth Syst. Sci. (2019) 128:110
https://doi.org/10.1007/s12040-019-1133-6

Impact of Cartosat-1 orography on weather prediction in a high-resolution NCMRWF unified model

Jisesh Sethunadh[1,*], A Jayakumar[1], Saji Mohandas[1], E N Rajagopal[1] and A Subbu Nagulu[2]

[1]*National Centre for Medium Range Weather Forecasting (NCMRWF), Ministry of Earth Sciences, Noida, India.*
[2]*National Remote Sensing Centre (NRSC), Balanagar, Hyderabad, India.*
**Corresponding author. e-mail: jiseshsethunadh@gmail.com*

MS received 27 May 2018; revised 19 October 2018; accepted 23 October 2018; published online 11 April 2019

The current study reports for the first time an application of orography from the Cartosat-1 satellite digital elevation model (DEM) generated at a source resolution of 30 m in a convection-permitting numerical weather prediction model. The effects of improvements in the representation of orography have been examined in the high-resolution regional National Centre for Medium Range Weather Forecasting (NCMRWF) Unified Model predictions for a heavy rainfall event over the city of Chennai. A time-lagged ensemble method is employed to account for the uncertainties associated with the initial conditions, which can better forecast extreme weather events than single forecasts. The simulations reveal that the predictions based on Cartosat-1 DEM capture the local details of the rainfall distribution better than the National Aeronautics and Space Administration shuttle radar topography mission DEM-based predictions, and better represent the orographic and thermal uplifting. The spatio-temporal patterns of the simulated rainfall over Chennai are superior in Cartosat-1 DEM-based simulations mainly due to the enhanced wind convergence and moisture transport. The present study reveals the role of mountains in the enhancement of heavy rainfall events over coastal cities and highlights the potential use of high-resolution orography in the improvement of the operational weather forecasting skill of the NCMRWF Unified Model.

Keywords. Orography; modelling; Cartosat-1; extreme rainfall; clouds; weather forecasting.

1. Introduction

Sporadic extreme rainfall events followed by devastating floods hit the South Indian city of Chennai on 1 December 2015, causing extensive damage to property and loss of life (Nagalakshmi and Prasanna 2016). Under synoptic conditions favourable to deep convective events, coastal cities near mountainous regions can experience intense rainfall events. Accurate high spatial-resolution predictions are needed for such cities for flood risk assessments and disaster management.

An improved representation of a mean orography field in the model will better simulate the effects of orography on flow fields, which will result in an improvement in the prediction skill of the model (Webster *et al.* 2003). These effects are largely due to the changes in the representation of the height, width and slope steepness of the mountains, which in turn affect the updraft speed in the simulations. Chennai city is located in the windward side of Jawadi hills of the Eastern Ghats, which modulates the northeasterly monsoon flow under the substantial influence of

orography. The effects of mountains in the vicinity of the coastal cities play a major role in determining the intensity and spatial pattern of heavy rainfall events (Houze 2012). Studies performed by Chen *et al.* (2013) over the northeastern Taiwan have also shown the importance of mountains in the enhancement of rainfall over the coastal regions. A detailed study performed by Phadtare (2018) highlights the role of the Eastern Ghats in the enhancement of extreme rainfall events over Chennai city. Hence, it is not possible to fully attribute the observed organisation and the extreme rainfall intensities over Chennai city to the intensity of the prevailing synoptic systems only (Chakraborty 2016; Van Oldenborgh *et al.* 2016; Krishnamurti *et al.* 2017; Phadtare 2018), as it is not sufficient to fully explain the observed heavy rainfall intensity over Chennai. The present study investigates the effects of improvements in the orography in an operational high-resolution regional weather forecasting model, which can substantially improve the skill of the numerical weather prediction (NWP) models. In order to accurately simulate the spatio-temporal structure of the extreme rainfall events, the regional weather prediction models should be able to reproduce the localised orographic effects in the simulations through the incorporation of high-resolution orography datasets.

Remote sensing techniques for gathering information about the orography have improved rapidly over the last few years, which offer several advantages like higher accuracy and increase in horizontal resolution. The mean elevation is the most fundamental field to represent orography in the models, which is explicitly resolved by the model grids. Here we have employed the regional version of National Centre for Medium Range Weather Forecasting (NCMRWF) Unified Model (NCUM-R) to simulate the extreme rainfall event. The NCUM-R is a high-resolution convective-scale model and the orographic effect in a high-resolution model is mainly felt through the resolved orography only (Webster *et al.* 2003). Hence, the main purpose of this paper is to elucidate the impact of resolved orography in an NWP model forecast over the coastal cities through the implementation of high-resolution Cartosat-1 digital elevation model (DEM) (Version-3R1 with 30 m horizontal source resolution) in the NCUM-R and by performing a case study of the Chennai floods using the ensemble technique.

2. Data and methodology

2.1 *NCUM-R orography from Cartosat DEM*

In this study, the predictions of the global NCUM model (N768) at a resolution of 17 km were downscaled to a 1.5 km horizontal resolution using the high-resolution regional model (NCUM-R), setup over a domain 73.25–87.25°E and 9.5–23.5°N. In the blending zone, the NCUM global model orography is slowly relaxed to the high-resolution NCUM-R grid by applying linear interpolation. GCMs using grid boxes of the order of tens of kilometres requiring orographic parameterisations to resolve the effects of sub-grid scale orography, whereas very high-resolution NCUM-R simulation can better resolve them explicitly, which reduces the requirement of sub-grid scale parameterisation. In the present study, the mean orography in the NCUM-R is represented using two datasets, National Aeronautics and Space Administration (NASA) shuttle radar topography mission (SRTM) DEM (here after SRTM DEM) and Indian Space Research Organisation (ISRO) Cartosat-1 DEM (here after Cartosat DEM). Simulations of NCUM-R are performed using SRTM DEM (source resolution of 90 m) and high-resolution Cartosat DEM (source resolution of approximately 30 m). SRTM DEM is available from the USGS website: www.usgs.org. Cartosat DEM high-resolution datasets have been digitally generated from Cartosat satellite observations by ISRO and these high-resolution Cartosat DEM (spatial resolution of 1 arcsec (approximately 30 m)) datasets are available in $1^\circ \times 1^\circ$ tile size on Bhuvan-geoportal of ISRO (http://bhuvan3.nrsc.gov.in/applications/bhuvanstore.php). From these raster tile files, the orography for the NCUM-R domain was generated by performing the following procedures.

The Cartosat-1 data is in the World Geodetic System 1984 (WGS 84) and the geoid undulations are computed (Rapp 1997) using spherical harmonic coefficients for Earth's gravitational potential data from the US National Geospatial-Intelligence Agency (NGA) web portal. These undulations are the separations between the geoid and WGS 84 ellipsoid, whose surface is equipotential. The geoid undulations corresponding to the latitude and longitude of each Cartosat-1 data points were used to correct the Cartosat-1 data values. The corrected data are then bi-linearly interpolated to the model grid. In the NCUM-R, the mean orography is improved by removing

sinks and spikes in the DEM by employing 1–2–1 filtering, which will help avoid the numerical instability and vertically coherent localised motions due to grid-scale spurious forcing (Webster *et al.* 2003; Sironi *et al.* 2015). The net effect of the applied smoother is a uniform weight over a 2×2 grid area. The same method has been applied for both SRTM DEM and Cartosat DEM. In addition to this, the default land–sea mask was also applied on both datasets.

There are many advantages of using Cartosat high-resolution orography data (horizontal resolution of 30 m) over relatively lower resolution SRTM orography data (horizontal resolution of 90 m), as the incorporation of high-resolution data can better reproduce the orographic effects in the NWP models. Cartosat DEM and deviations of Cartosat DEM from SRTM DEM over the model domain are depicted in figure 1(a and b), respectively. Few studies have compared both DEMs, which show that Cartosat DEM has higher accuracies in highly rugged terrains and valleys over the Indian domain (Yarrakula *et al.* 2013; Arun *et al.* 2016; Baral *et al.* 2016). Figure 1(b) clearly shows large areas having significant difference between Cartosat DEM and SRTM DEM over Chennai city, which can have a direct impact on the precipitation simulated over these regions. The mean errors of the DEMs generally increase with an increase in the elevation value (Yadav and Indu 2016), which also depends on the land use and land cover (LULC) characteristics of the region. The mountain peaks in the Jawadi hills region and Western Ghats region in both DEMs in the model grids are depicted in figure 2, which clearly show the finer details resolved in Cartosat DEM. Spot heights comparison studies performed by Baral *et al.* (2016) have found that SRTM DEM shows significant deviations in the rugged terrains (e.g., Kanchenjunga area (27.70°N and 88.14°E)). Similar to this, the SRTM DEM shows significant deviations from Cartosat DEM over the hilly regions in the model domain (see figure 1b). The present study focuses on the orographic effects of the Jawadi hills (12.15–12.40°N; 78.2–79.10°E) of the Eastern Ghats, located to the southwest of Chennai city at a distance of approximately 200 km. These hills have a length of about 60 km and width of about 25 km with an average height of 1053 m above the mean sea level. A special feature of these hills is that there is a plateau at the top with an extent of 10 km. The extent of the hills and the slope of the plateau at the top also play a role in the generation of rainfall over the regions near the hills (Sato 2013). SRTM DEM can represent the mountains in the model domain, but a higher resolution Cartosat DEM better represents the mountain peaks and slopes in the model domain.

2.2 *Modelling and verification strategy*

In the present study, we have employed the NCUM-R (Jayakumar *et al.* 2017) to simulate the extreme rainfall event that occurred over Chennai city. The model is based on Even Newer Dynamics for General Atmospheric Modelling of the Environment (END Game) dynamical core (Wood *et al.* 2014) with a radiation scheme based on Edwards

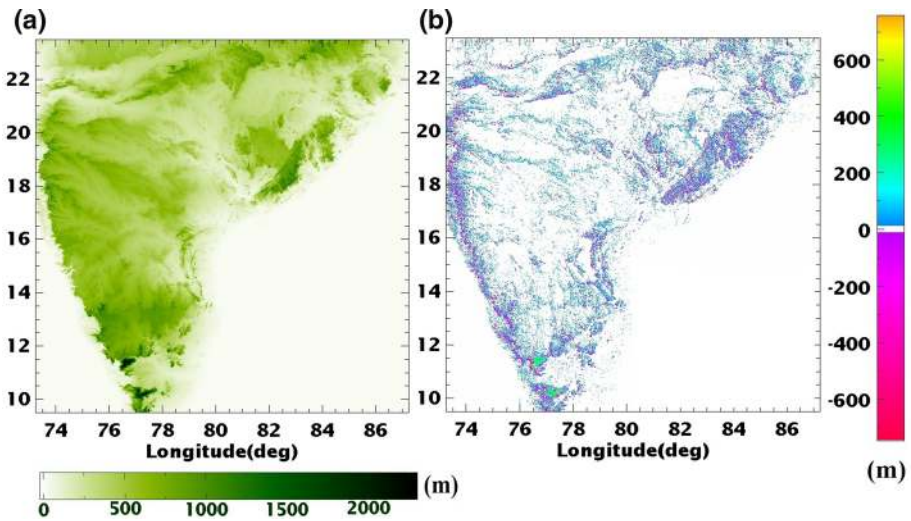

Figure 1. Orography representation over the model domain: (**a**) Cartosat-1 DEM data and (**b**) the difference between Cartosat-1DEM and SRTM DEM. The colour scale shows terrain elevations in metres.

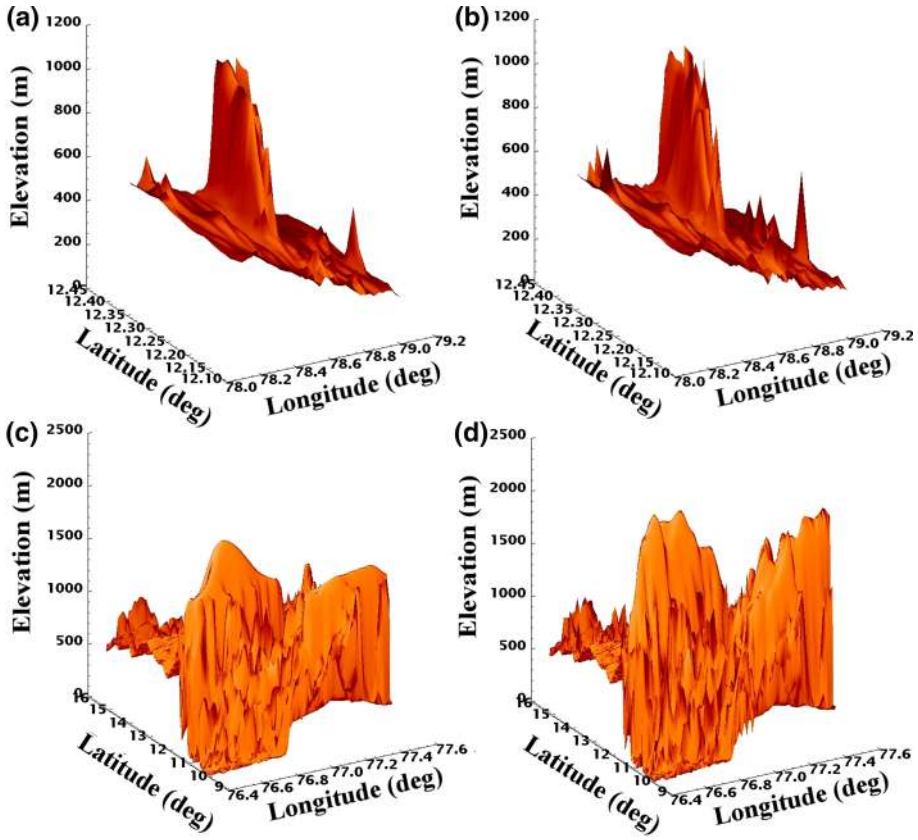

Figure 2. NCUM-R model grid orography of Jawadi hills using (**a**) SRTM DEM and (**b**) Cartosat-1 DEM, and Western Ghats using (**c**) SRTM DEM and (**d**) Cartosat-1 DEM.

and Slingo (1996), precipitation/microphysics based on the modified Wilson and Ballard (1999) scheme (Walters *et al.* 2017) and has a cloud scheme based on that of Wilson *et al.* (2008). The convection-permitting NCUM-R allows to explicitly resolve the mid- and deep-level convection, and the shallow convection in the model is parameterised using the scheme of Gregory and Rowntree (1990). A grey-zone blended planetary boundary layer (PBL) scheme (Boutle *et al.* 2014) is used in the NCUM-R and the land surface characteristics over the model domain are generated from the ISRO LULC data (Unnikrishnan *et al.* 2016). In the present study, the improvement in the representation of the resolved mean orography in the model is achieved by the implementation of high-resolution Cartosat DEM and its implications on the predictions of rainfall, wind and cloud systems are discussed in the following sections.

In order to assess the ability of NCUM-R to simulate extreme rainfall events, a time-lagged ensemble technique (Hoffman and Kalnay 1983) with different forecast lead times is used in this study. Short-range predictions generally show a strong dependency on initial conditions. The variations in initial conditions in the ensemble simulation represent the uncertainty in the initial conditions and approximations in the deterministic forecast. The time-lag ensemble technique decreases the inconsistencies present in the simulations. Nevertheless, the selected case is a single high impact extreme rainfall event with a prevailing cyclonic system, the time-lagged ensemble technique will provide a better understanding of the mechanism behind the enhanced rainfall event that occurred on 1 December 2015 than performing another case study of a heavy rainfall event that occurred over Chennai with a much different synoptic situation. The use of the ensemble technique would allow us to increase the robustness of the results of this study by addressing the uncertainty in the model simulation through variations in the initial conditions. In the present study, we have used the operational configuration of NCUM-R at NCMRWF and produced a five-member ensemble of three-day predictions with the initialisation cycles separated sequentially at 6 hr (00 Universal Time Coordinated (UTC), 06 UTC, 12 UTC

and 18 UTC) from 29 November 2015, 18 UTC. Here we did not consider the ensemble members with initial conditions less than 12 h lead time as it will not allow the model to evolve properly and the forecasting skill will be less. This is justifiable as earlier studies employing operational weather models with three ensemble members were found to be showing improved forecasting skills (Vogel *et al.* 2014). Time-lagged ensemble simulations using both SRTM DEM (hereafter SRTM-run) and Cartosat DEM (hereafter Cartosat-run) orography datasets were performed and predictions from each ensemble members were examined. We have produced ensemble mean for the diagnosis, which will help average out the effects of natural variability (the chaotic nature of the atmosphere) from independent runs and will help elucidate the impact of orography.

The verification of NCUM-R forecasts against hourly rainfall data from Japan Aerospace Exploration Agency (JAXA) Global Satellite Mapping of Precipitation (GSMaP) observations and integrated multi-satellite retrievals for GPM (IMERG) were performed to assess the forecasting skill of the SRTM-run and Cartosat-run. In addition, the model forecasts were also verified using rain gauge observations at Chembarambakkam station (13.00°N and 80.03°E) (Narasimhan *et al.* 2016) located near Chennai city (hereafter rain gauge) to increase the accuracy of the results.

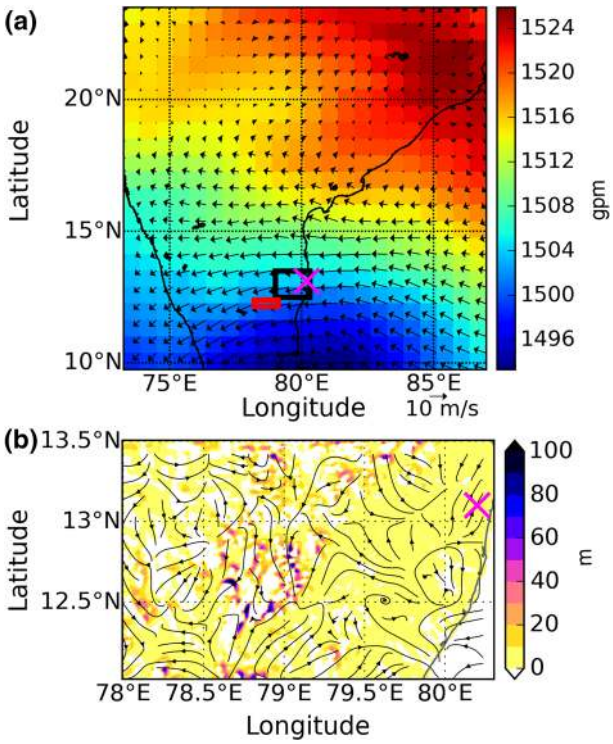

Figure 3. (**a**) ERA-Interim reanalysis of 850 hPa winds (vector, m/s) overlaid by geopotential heights (shaded, gpm) for 1 December 2015 at 12:00 UTC. The Chennai domain (black box), location of Jawadi hills (red box) and Chennai city location (marked 'X' in magenta) are also given; (**b**) the difference in magnitude of orography generated in the NCUM-R using Cartosat-1 DEM and SRTM DEM (only positive values are shown here) (shaded, m) and the difference in ensemble mean of 50 m wind (streamlines) simulated in the NCUM-R over Chennai city (Chennai city location is marked as 'X').

3. Synoptic situations

During the northeast monsoon season, the southeastern coast of India experiences extreme rainfall events due to the formation of cyclonic storms over the Bay of Bengal. On 30 November 2015, a well-marked low-pressure area was observed over the Bay of Bengal and it quickly intensified into a cyclonic storm on 1 December 2015, resulting in heavy rainfall over the southeastern coastal regions of India. Precipitation amounts up to 60 mm/h were recorded at Chembarambakam rain gauge station. The ERA-Interim reanalysis data illustrated in figure 3(a) shows the synoptic situation prevailed over Chennai city on 1 December 2015 at 12 UTC. The ERA-Interim 850 hPa geopotential height shown in figure 3(a) clearly shows a cyclonic system associated with a low-pressure system over the Bay of Bengal indicated by lower values of geopotential. It is evident from the figure that the prevailing winds over Chennai city were easterly, which transport moisture to the Chennai region. The heavy rainfall that occurred over Chennai was related to this persistent cyclonic system and associated moisture transport from the Bay of Bengal. Heavy rainfall associated with orographic enhancement of precipitation is quite often seen over the coastal regions, where mountains/hills are present in the vicinity of coast (Chen *et al.* 2013).

4. Results and discussions

4.1 *Impact of orography on weather prediction*

The orographic effects are known to influence the magnitude and distribution of precipitation in mountainous regions, which are highly dependent on the characteristics of the mountain ranges. There exists a number of modelling studies about the sensitivity of simulated orographic rainfall to

the horizontal resolution of the model, and earlier studies have already shown that the rainfall simulation over the windward side of slopes improve with improvements in the representation and resolution of the model orography (Dimri 2004; Smith *et al.* 2015). In the present study, the effects of representation of mean orography using SRTM DEM and Cartosat DEM were studied, which show large differences in heights and slopes of mountains in the domain of interest (figures 1b and 2). The domain has a very rugged orography characterised by closely spaced mountains with a wide range of scales and shapes, which favours the formation of different types of clouds. The presence of rugged orography can affect the spatio-temporal structure of the precipitation near the hilly regions as the intensity of orographic precipitation due to low height mountain ranges is roughly proportional to the altitude of the hills and prevailing wind speed (Jiang 2003). It is evident from figure 3(b) that the difference in Cartosat DEM and SRTM DEM has a high impact on low-level (50 m) wind. The figure clearly shows Jawadi hills (over the region 79.5°E and 12.75°N) as a source of wind diversion near the Jawadi hills region. This leads to a wind convergence over Chennai city from the southwesterly direction and northeasterly direction from the Bay of Bengal, which can modify the local weather over the Chennai region. In addition, small changes in orography can be seen all over the domain which can alter the channelling of air flow and contributes to the improvement in simulations.

The NCUM-R model employed in this study has explicit convection, which very well represents the transport of heat, moisture and momentum associated with the convective motions. Figure 4(a and b) shows the model surface temperatures at 1.5 m (shaded) and 850 mb wind (vectors) from the SRTM-run and Cartosat-run, respectively, on 1 December 2015 at 6 UTC. The differences between these fields from the SRTM-run and the Cartosat-run from 6 to 12 UTC are depicted in the rest of the panels. In addition to the prevailing easterlies in the domain, the Cartosat-run produced enhanced moisture transport towards the regions 12.5–13.5°N and 79.0–80.3°E (hereafter referred to as the Chennai domain). This causes wind convergence near the domain, and a fluid parcel which converges horizontally becomes more cyclonic. As a result, a cyclonic vortex starts to form northeast of the Chennai domain. Figure 4(d–f) shows the temporal evolution of the cyclonic vortex and a gradual intensification of the cyclonic system can be clearly seen in figure 4(d–f), which has a maximum at 9 UTC. The formation of a low-pressure system during the heavy rainfall event is in synergy with the results of the study performed by Phadtare (2018). The difference in the Cartosat-run and the SRTM-run shown in figure 4(g–i) clearly shows the weakening of the cyclonic vorticity from 10 UTC onwards over the northeast part of the Chennai domain as the precipitation over these regions intensify. The weakening of cyclonic vorticity is mainly due to the decrease in wind convergence and moisture transport near the Chennai domain. In addition to wind convergence, figure 4(c–f) reveals that the Cartosat-run produced higher surface temperatures near Chennai city when compared to the SRTM-run, and figure 4(g–i) shows that the difference in temperature decreases as the amount of rainfall increases over the domain (see figure 10). Higher surface temperatures will enhance the convection associated with surface heating, and lead to the formation of clouds as it causes air mass to lift, expand and cool until it reaches saturation. The latent heat released due to moisture condensation enables many flows to rise over mountains (Jiang 2003). In addition to the increase in surface temperatures, the reduction in temperatures can also be seen over the region near 78°E–15°N, which can be attributed to the lapse-rate associated with the increase in mountain height in Cartosat DEM when compared to SRTM DEM. Furthermore, the cloud formation due to mountain uplifts also leads to the reduction in surface temperatures on the slopes (Kitoh 1997). Studies have also shown that the magnitude of cyclone-induced moisture transport has a strong dependence on the meridional temperature gradient (Boutle *et al.* 2011), which in this case also helps to intensify the cyclonic vorticity developed near the Chennai domain.

The improvements in orographic representation over the domain have a direct effect on the water vapour transport over the Chennai domain. The magnitude of moisture flux transport in the simulations with SRTM DEM and Cartosat DEM is illustrated in figure 5(a and b), respectively, where the magnitude of vertically integrated moisture transport (VIMT) from the surface to 500 hPa is illustrated as the shaded region and the vertically integrated moisture flux (VIMF) as vector. The vertically integrated zonal and meridional flux components can be calculated as

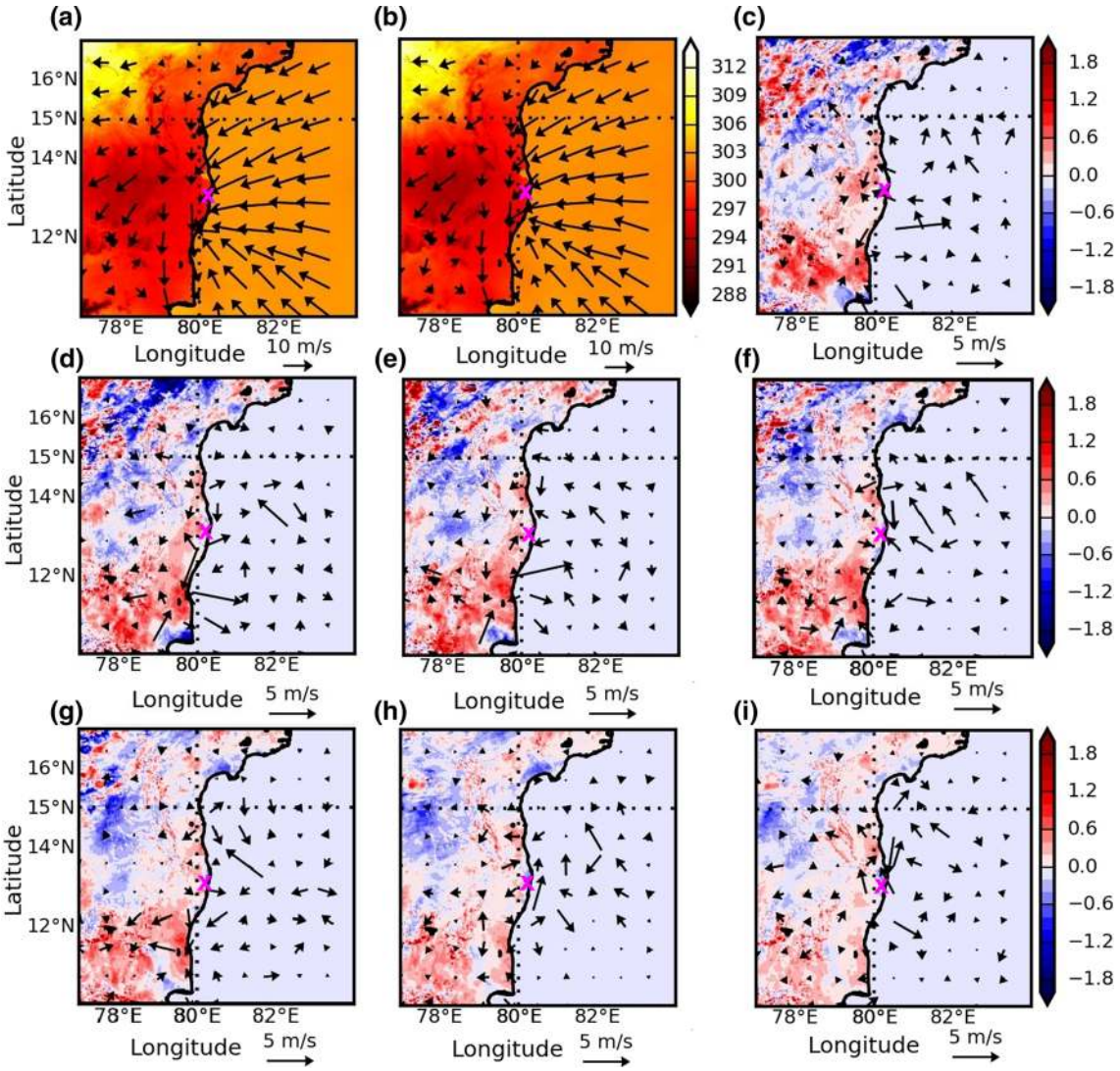

Figure 4. Surface temperatures (shaded, K) and 850 mb winds (vectors, m/s) at 6 UTC on 1 December 2015 in SRTM-run and Cartosat-run are shown in (**a**) and (**b**), respectively. The differences in Cartosat-run and SRTM-run at 6, 7, 8, 9, 10, 11 and 12 UTC are shown in (**c**–**i**), respectively.

$$Q_u = \frac{1}{g}\int_p^{p_s} qu \, \mathrm{d}p, \tag{1}$$

$$Q_v = \frac{1}{g}\int_p^{p_s} qv \, \mathrm{d}p, \tag{2}$$

where g is the gravity, q is the specific humidity, u is the zonal component of the wind, v is the meridional component of the wind, p_s is the surface pressure and p is 500 hpa pressure. Figure 5(c) shows the difference in VIMT and VIMF between the Cartosat-run and the SRTM-run. The differences in VIMT vectors overlaid in figure 5(c) depict the enhanced northeasterly moisture transport towards Chennai city in the Cartosat-run compared to SRTM-run. Studies performed by Chen *et al.* (2013) have shown that the amount of low-level moisture and orographic effects is equally important for a heavy rainfall event near mountains. It is clear that low-level convergences occurred in this case and the predominant northeasterly winds transported moisture to the Chennai region, which caused thunderstorms and sporadic heavy rainfall events. Figure 2 clearly illustrates that the Cartosat DEM has more number of higher peaks than that of SRTM DEM, which improves the simulated wind patterns and moisture transport over mountainous regions. Changes in slopes and altitudes of elevated landform in the model can cause a change in the air flow and moisture transport. This will eventually alter the convergence of air and frontal lifting in the model, which directly affects the rainfall prediction over the domain.

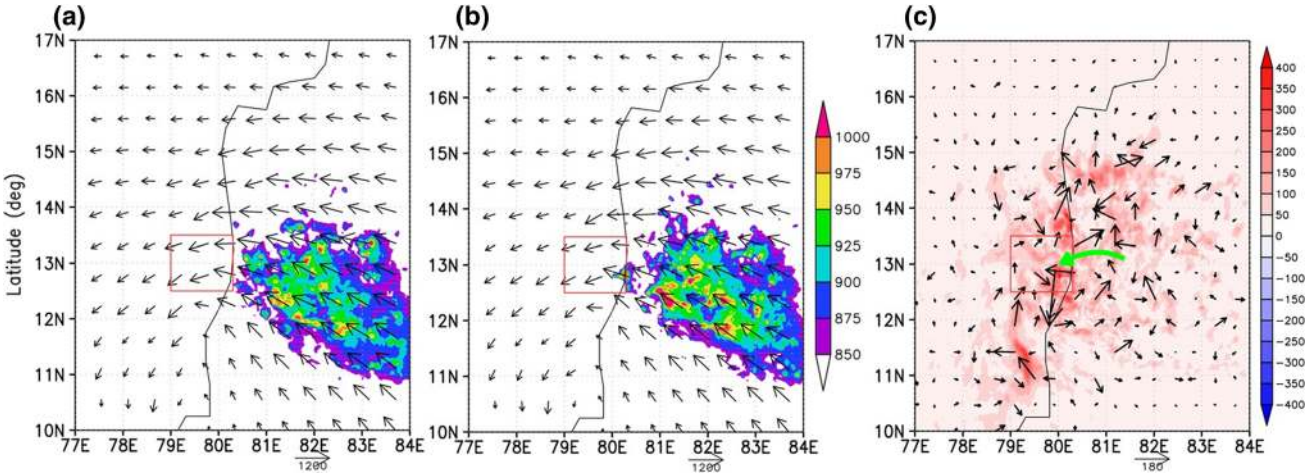

Figure 5. Magnitude of VIMT from the surface to 500 hPa and moisture transport (shaded, kg/m/s) (values above 700 kg/m/s are shown here) and VIMF vectors (kg/m/s) in the time-lagged ensemble forecast at 9 UTC on 1 December 2015 in (**a**) SRTM-run, (**b**) Cartosat-run and (**c**) the difference in magnitude of VIMT (shaded) and VIMT vectors in Cartosat-run and SRTM-run.

The magnitude VIMT and VIMF vectors at 9 UTC on 1 December 2015 illustrated in figure 5(a and b) reveals that the rainfall peaks observed over Chennai city are associated with the orographic uplifting in the vicinity of the coastal city due to the prevailing northeasterly winds and anomalous cyclonic systems present over the Bay of Bengal. Since the peak rainfall in the model is found to be around 12 UTC, we have performed a detailed analysis of VIMT and VIMF with a lead time of 3 h (9 UTC) as the synoptic-scale low-pressure systems that is prevalent over the Bay of Bengal can draw moisture from regions within a distance of about 3–5 times the radius of the system (Trenberth *et al.* 2003). Figure 5(a and b) shows regions with major moisture transport and high wind speed pathways associated with the cyclonic system, which are directed to the Chennai domain. A vector analysis indicates that the moisture transport from the Bay of Bengal that converged over the eastern parts of the Chennai domain is bringing moisture to the Chennai domain. It is evident from figure 5(c) that the Cartosat-run produces higher values of VIMT over the coastal regions of the Chennai domain and shows stronger flow patterns of VIMF towards the coastal regions of the Chennai domain (the continual flow pattern of VIMF towards the Chennai domain is indicated by a green arrow). These conditions favour the cloud formation as the type of cloud that formed depends on the availability of moisture and stability of the atmosphere, which would cause enhanced rainfall over the domain. Hence, the observed heavy rainfall event can be better predicted with improved orographic representation, which will result in an enhanced moisture transport (figure 5c) and associated cloud formation over the domain. A comparison of figure 5(a and b) indicates that the improvement in orography has contributed to an intensification of moisture availability over the southwest Bay of Bengal by perturbing the prevailing synoptic scale system, which also contributed to the shifting of rainfall patterns from the ocean to land as seen in figure 5(c).

The difference in ensemble mean of 850 hPa geopotential heights over the Chennai domain at 6 UTC (left panel) and 12 UTC (right panel) on 1 December 2015 shown in figure 6(a and b) displays an increase in the geopotential height in the Cartosat-run when compared with the SRTM-run, depicting an increase in the easterly wind towards the Chennai region with time. The increase in the geopotential height in the Cartosat-run (figure 6b) over the Chennai region shows the presence of warm air masses. The signatures of the cyclonic vorticity formed over the northeastern side of the Chennai domain can be seen as a blue colour patch in figure 6(a) at 6 UTC, which indicates a decrease in geopotential height in the Cartosat-run when compared with the SRTM-run. At 12 UTC, the difference in geopotential over the Chennai domain increases, which clearly shows the presence of warm air masses over the domain. The changes in orography have an effect on the vertical velocity as shown in figure 6(c and d), which show regions with higher values of vertical velocity indicating enhanced vertical velocity in the Cartosat-run in comparison with the SRTM-run.

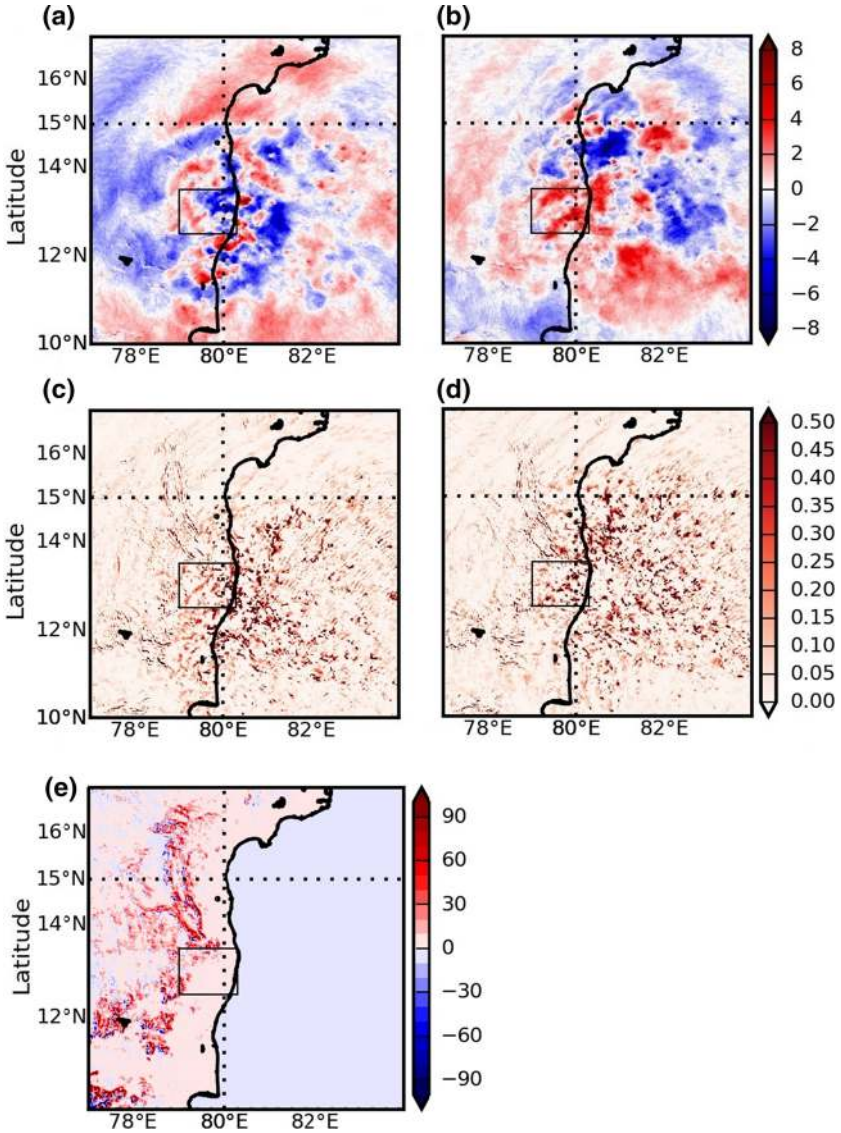

Figure 6. Difference in ensemble mean of simulations at 6 UTC (left panel) and 12 UTC (right panel) on 1 December 2015 in CARTOSAT-run and SRTM-run at 850 hPa. Panels (**a**) and (**b**) show geopotential height (gpm), and panels (**c**) and (**d**) show vertical velocity (m/s) (only positive values of vertical velocity are shown here for clarity). Panel (**e**) shows the difference in Cartosat-1 DEM and SRTM DEM.

Though the high values of vertical velocity seen in individual ensemble members are not well reproduced in figure 6(c and d) due to the ensemble mean calculation, the figures clearly show a spatial correlation between the geopotential difference and vertical velocity difference over the Chennai domain. The difference in orography height in the Cartosat-run and the SRTM-run is shown in figure 6(e) which indicates a weak positive correlation with the positive vertical velocity shown in figure 6(c and d).

In order to find out the effect of orography on simulated clouds in NCUM-R, we have performed a histogram comparison of clouds simulated in the SRTM-run and the Cartosat-run over the Chennai domain and the results are depicted in figure 7. The low-level cloud cover (surface 6000 ft) simulated in the Cartosat-run shows a significant increase in the cloud fraction in the bins between 0.5 and 0.9, which indicates the supremacy of Cartosat-runs in simulating the enhanced cloud cover over the Chennai domain. This result is in synergy with the histogram analysis of rainfall shown in figure 9, as the enhanced cloud cover under favourable conditions positively correlates with the amount of rainfall. Earlier works have identified that the cloud cover has a positive correlation with relative humidity and vertical velocity (Walcek 1994). The larger values of vertical velocity seen in figure 6(c and d) cause the air mass to be lifted and cooled

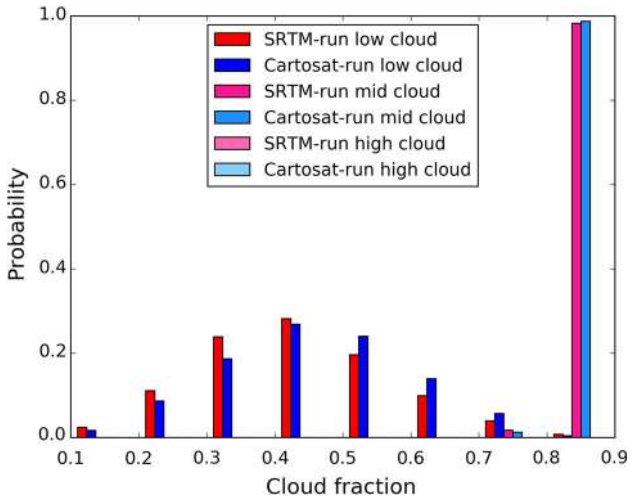

Figure 7. Histogram comparison shows normalised probability density function of low level, mid-level and high level cloud fraction over the Chennai domain at 12 UTC on 1 December 2015 in SRTM-run and Cartosat-run.

to its dew point, and eventually become saturated with cloud droplets and enhance the cloud formation. As the air mass cools down adiabatically, the relative humidity increases and forms a cloud when it reaches 100%. A detailed analysis of relative humidity in the simulations (figures not shown) shows an increase in relative humidity over the Chennai domain in the Cartosat-run when compared with the SRTM-run. The cloud size is also linked to the vertical velocity through the entrainment process, which has a strong dependence on the vertical velocity present below the cloud base and has a direct effect on the precipitation patterns. These factors support enhanced cloud formation in the Cartosat-run than in the SRTM-run over the Chennai domain. This enhanced cloud formation also caused an increase in the precipitation over the Chennai domain at 12 UTC. Hence, the Cartosat-run is better reproducing the heavy rainfall events over the Chennai domain, favoured by the cyclonic circulation formed over the north-eastern parts of the Chennai domain due to the combined effects of improvements in the orographic uplifting and thermal forcing.

Histogram comparisons of mid-level clouds (~6000–18,000 ft) and high-level clouds (above 18,000 ft) are showing a maximum in the higher cloud fraction bins. The mid-level clouds simulated using the Cartosat-run and the SRTM-run during the heavy rainfall event show significant differences in the bins ranging from 0.8 to 0.9, which indicate that there could be significant differences in the simulated mixed-phase clouds (MPCs) causing a difference in mid-level cloud fraction. MPCs consist of supercooled liquid water droplets and ice crystals. Earlier studies have shown that the orographic MPCs are frequently observed in mountainous regions (Henneberg *et al.* 2017). MPCs are supposed to be short lived because the difference in the saturation vapour pressure of ice crystals and water droplets causes the rapid growth of ice crystals at the expense of water droplets and enhances precipitation. Studies performed by Jayakumar *et al.* (2017) have already shown that the MPCs are not well simulated in the NCUM-R. Furthermore, high-level clouds in the Cartosat-run and the SRTM-run are not showing any significant differences over the Chennai domain. Hence, a detailed study of NCUM-R using the Cloud Feedback Model Intercomparison Project (CFMIP) Observation Simulator Package (COSP) and its verification using satellite observations is required to get a deep insight into the effects of orography on MPCs in NCUM-R, which is beyond the scope of this study.

4.2 *Simulation of the heavy rainfall event using NCUM-R*

The impact of orography on the heavy rainfall event which occurred over Chennai city on 1 December 2015 is examined in this section. Figure 8 shows the spatial distribution of ensemble mean rainfall based on the SRTM-run and the Cartosat-run (figure 8c and d) along with IMERG and JAXA observations in figure 8(a and b). The JAXA observations, in general, have issues in measuring precipitation over the ocean (Aonashi *et al.* 2009), which could be the reason for high values of precipitation seen over the ocean in figure 8(b) when compared to figure 8(a). Evaluation studies performed by Ning *et al.* (2017) have shown that JAXA observations have a tendency to overestimate light rainfall, whilst IMERG observations have a tendency to underestimate 8–64 mm/day rainfall. A comparison of simulated rainfall in Cartosat-run and SRTM-run shows that the Cartosat-run is in better agreement with the rainfall observations over the coastal regions of Chennai city, especially over the region near 14.0°N and 80.0°E, where the SRTM-run shows very little rainfall when compared with the observations. This is in agreement with the increase in mountain heights seen in Cartosat DEM over the northern and western sides of the Chennai domain (see figure 6e). Earlier studies have shown that an enhancement in rainfall can occur over hundreds of kilometres away from the mountains when

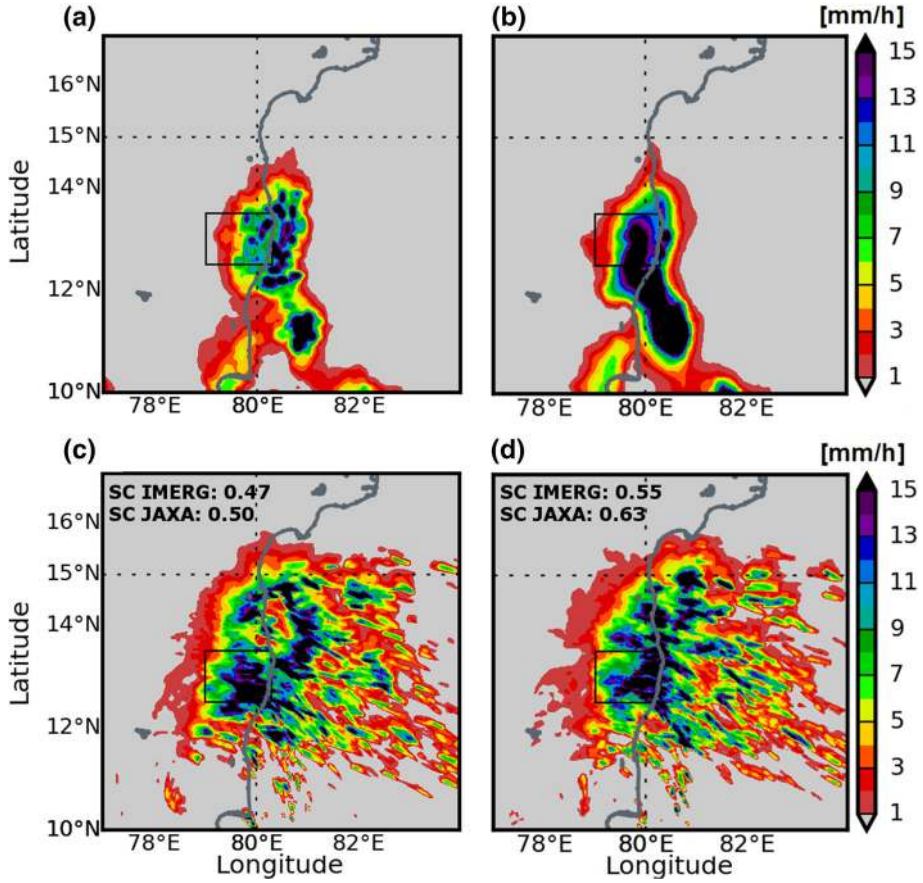

Figure 8. Observed hourly rainfall valid at 12 UTC on 1 December 2015 from (**a**) IMERG and (**b**) JAXA, and time-lagged ensemble predictions in (**c**) SRTM-run and (**d**) Cartosat-run data. Spatial correlation between the simulations with GPM IMERG (SC IMERG) and JAXA (SC JAXA) over the Chennai domain (black box) are also given.

orographically blocked flow occurs (Houze 2012; Phadtare 2018). The SRTM-run shows a shift in moderate to heavy rainfall patterns over the ocean, which is very much improved in the Cartosat-run. The heavy rainfall patterns simulated in NCUM-R over Chennai city in the Cartosat-run is a better match with observations, which is in good agreement with large clouds seen over Chennai city in the Cartosat-run (figure 7). Moreover, the bias in rainfall over the ocean is less in the Cartosat-run when compared with the SRTM-run (e.g., region near 14.5°N and 82.5°E). The spatial correlations (SC) between the simulations with GPM IMERG (SC IMERG) and JAXA (SC JAXA) over the Chennai domain (black box) are also tabulated in the respective figures (see figure 8c and d). As the observed maximum of the accumulated rainfall over land was found to be near Chennai city, we have computed the spatial correlation over the Chennai domain. The SC of the SRTM-run and the Cartosat-run against IMERG over the Chennai domain at 12 UTC is found to be 0.47 and 0.55, respectively. Similarly, against JAXA, SC gives about 0.50 and 0.63. Verification against both observational datasets shows the supremacy of the Cartosat-run over the SRTM-run. Further analysis shows that the localised features of rainfall over the Chennai domain are more evident in the Cartosat-run, which is largely contributed by the shift in rainfall from the ocean to the land over the eastern coast of Chennai city. Histograms of the simulated rainfall data provide considerably more information about the distribution of the rainfall amount (figure 9). Histogram comparison of the Catosat-run and the SRTM-run with IMERG and JAXA observations over the domain 12.0–15.0°N and 79.0–82.0°E shows a marginal improvement in rainfall simulation in the Cartosat-run below 11 mm/h and a significant improvement in rainfall prediction above 11 mm/h bins. The number of occurrences of moderate–heavy rainfall (11–16 mm/h) amount over the domain is found to be more in the Cartosat-run when compared with the SRTM-run. This clearly indicates that there is an enhancement of rainfall over the Chennai domain due to the implementation

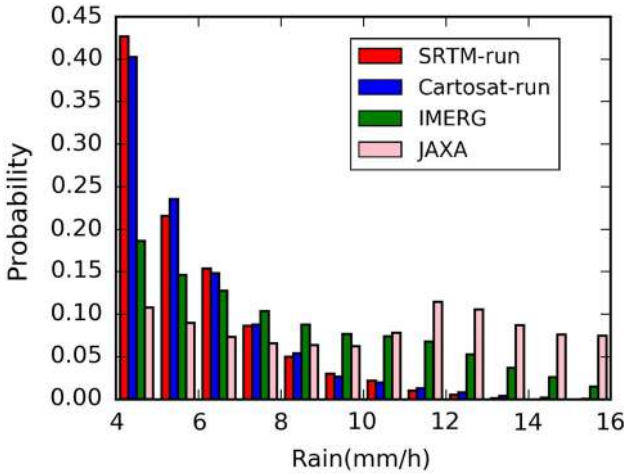

Figure 9. Histogram comparison depicting normalised probability density function at each bin for 12 UTC rainfall (mm/h) on 1 December 2015 over the Chennai domain in SRTM-run (red), Cartosat-run (blue), GPM IMERG (green) and JAXA Global Rainfall Watch observations (magenta).

of high-resolution Cartosat DEM in NCUM-R. Conversely, 5–6 mm/h rainfall comparison shows that it is slightly overestimated in the Cartosat-run. The light rainfall (4–5 mm/h) occurrences are also better simulated in the Cartosat-run than the SRTM-run.

The time series of the hourly accumulated rainfall amount from the ensemble mean of simulations using SRTM DEM and Cartosat DEM are compared with the available rain gauge observations from Chembarambakkam station, which is depicted in figure 10(a). The amount of rainfall during the peak spell period (9–15 UTC) from the SRTM-run and the Cartosat-run is found to be 12.42 and 17.28 mm/h, respectively, whereas the observed amount is 29.85 mm/h. Rainfall prediction at this gauge location is found to be improved by ∼4.79 mm/h and the correlation between the two time series (C) is improved by 0.3452 in the Cartosat-run when compared to the SRTM-run. Hence, it can be concluded from figure 10(a) that there is a significant improvement in the phase and magnitude of the extreme rainfall prediction with the implementation of Cartosat DEM in NCUM-R. In addition to the rain gauge observation, we compared the domain averaged rainfall over Chennai with the satellite observation also (figure 10b). It can be seen from figure 10(b) that the intensity of ensemble mean rainfall forecast is better simulated in the Cartosat-run when compared to the SRTM-run during the peak hours and the figure also illustrates significant improvements in the phase

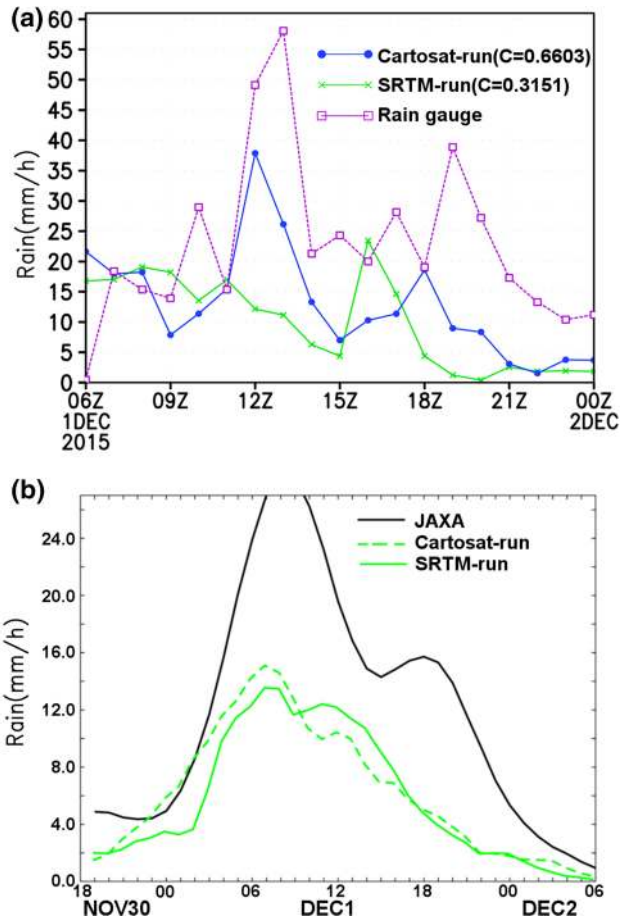

Figure 10. (**a**) Observed hourly rainfall at Chembarambakkam rain gauge and simulated hourly rainfall in SRTM-run and Cartosat-run at model grids close to the Chembarambakkam rain gauge station. (**b**) Simulated domain mean rainfall over the Chennai domain in the Cartosat-run (dashed lines) and SRTM-run (solid line) along with JAXA Global Rainfall Watch observations over the Chennai domain.

of the simulated rainfall in the Cartosat-run when compared with the SRTM-run on 1 December 2015.

5. Conclusions

The present study reports, for the first time, the use of Cartosat-1 satellite DEM for generating orography for the NCUM-R, and the effects of orography on rainfall, wind and cloud systems are studied. The study is focused on the impact of mean orography generated from high-resolution Cartosat-1 DEM and SRTM DEM on the NCUM-R simulation of an extreme rainfall event that occurred over Chennai city under prevailing cyclonic conditions during the northeast monsoon period. Time-lagged ensemble method with varying initialisation cycles were used to average out the effects of natural

variability and to elucidate the impact of orography on rainfall prediction. Spatial and temporal correlation analysis against rain gauge and satellite observations showed that there is a significant improvement in the phase and magnitude of heavy rainfall episodes in the Cartosat-run and it captures the local details of the rainfall distribution over the Chennai domain better than the SRTM-run. The simulations revealed that the orographic effects of Jawadi hills have significantly contributed to the localisation and enhancement of rainfall. A histogram analysis of simulated and observed rainfall amount showed that the number of occurrences of moderate to heavy rainfall is better predicted in the Cartosat-run. Enhanced moisture transport with changes in the uplift upstream has resulted in an enhanced rainfall on the windward side of the Jawadi hills, and led to a reduction in the moisture availability on the leeward side. It was also found that a positive moisture transport in the Cartosat-run triggered a localised meso-scale system by creating surface instability in the boundary layer, which in turn caused an enhancement in precipitation.

The study also revealed that the extreme rainfall event was not necessarily a manifestation of the synoptic system only, but the perturbation of the synoptic system by orography through wind diversion and uplifting, which brought more warm moist air to the land and contributed to the enhancement of rainfall. As a result of this synoptic scale perturbation, the rainfall over the ocean was shifted slightly into the land. Results show that a change in wind caused by a change in the mountain dimension can perturb the large-scale synoptic systems, which can in turn change the rainfall patterns associated with the cyclonic system, and ultimately lead to a reduction in land–ocean rainfall bias in the model. At larger scales, a change in the mean orographic slope can cause a change in wind direction to conserve potential vorticity of the flow (Lott 1999). The predominant large-scale low-level winds were northeasterly and this indicates that the moisture transport from the Bay of Bengal to the land will change with the change in the orographic slope and result in an increased orographic rainfall under the right conditions. The model has a terrain following a geometric height-based vertical co-ordinate system, hence the pressure gradient will change with the surface slope and results in modified flow fields. These effects also play a major role in rainfall forecast, which were improved in the model by the use of high-resolution Cartosat DEM. Hence, the prediction of heavy rainfall events in the vicinity of mountains using NCUM-R demands high accuracy in mountain heights and slopes in orography. As a result of the incorporation of high-resolution Cartosat-1 DEM in the NCUM-R, the simulations show more clouds over the Chennai region than SRTM-run. This is mainly due to the enhanced wind convergence and moisture transport over the Chennai domain due to the improvements in the orographic uplift and thermal uplift. These improvements lead to a better prediction of rainfall over the Chennai domain. This is evident from the correlation calculations with satellite observations, which show a higher spatial correlation in the Cartosat-run when compared with the SRTM-run. Furthermore, rainfall forecast verification using the Chembarambakkam rain gauge station shows an improvement of $\sim$4.79 mm/h and a histogram analysis reveals that the number of occurrences of moderate–heavy rainfall over the Chennai domain has improved in the Cartosat-run, which is in synergy with the histogram analysis of simulated cloud fractions. Therefore, we may hypothesise that the amount, location and phase of the rainfall patterns over the model domain are highly improved by the improvements in the mountain dimensions and slope, which in turn resulted in an improvement in the prediction skill of NCUM-R. This improvement in the prediction skill of NCUM-R will help improve the disaster management and flood area assessments in India.

The skill of the currently employed ensemble prediction method can be improved by the use of a convective scale ensemble prediction system, which accounts for the model errors such as the errors introduced by the initial condition (IC), lateral boundary condition (LBC), model physics, etc. However, such an ensemble system at a high-resolution regional scale was not available at NCMRWF during the study period. It is envisaged that future work will employ the convective scale ensemble prediction systems, including sub-grid scale orographic effects using Cartosat-1 DEM and the evaluation of mixed phase clouds simulation using COSP with satellite observations.

Acknowledgements

The authors gratefully acknowledge Dr Stuart Webster, Met Office, UK, for his valuable comments and discussions. They acknowledge the data

source CartoDEM Version-3 R1, National Remote Sensing Centre, ISRO, Government of India, Hyderabad, India, NASA for the SRTM and GPM IMERG products and the JAXA GSMaP rainfall product.

References

Aonashi K, Awaka J, Hirose M, Kozu T, Kubota T, Liu G, Shige S, Kida S, Seto S, Takahashi N and Takayabu Y N 2009 GSMap passive microwave precipitation retrieval algorithm: Algorithm description and validation; *J. Meteorol. Soc. Japan Ser. II* **87A** 119–136, https://doi.org/10.2151/jmsj.87A.119.

Arun P, Katiyar S K and Prasad V 2016 Performances evaluation of different open source DEM using differential global positioning system (DGPS); *Egypt. J. Remote Sens. Space Sci.* **19**(**1**) 7–16, https://doi.org/10.1016/j.ejrs.2015.12.004.

Baral S S, Das J, Saraf A K, Borgohain S and Singh G 2016 Comparison of Cartosat, ASTER and SRTM DEMs of different terrains; *Asian J. Geoinformatics* **16**(**1**) 1–7.

Boutle I A, Belcher S E and Plant R S 2011 Moisture transport in midlatitude cyclones; *Quart. J. Roy. Meteor. Soc.* **137** 360–373, https://doi.org/10.1002/qj.783.

Boutle I A, Eyre J E J and Lock A P 2014 Seamless stratocumulus simulation across the turbulent grey zone; *Mon. Weather Rev.* **142** 1655–1668.

Chakraborty A 2016 A synoptic-scale perspective of heavy rainfall over chennai in November 2015; *Curr. Sci.* **111**(**1**) 201–207, https://doi.org/10.18520/cs/v111/i1/201-207.

Chen C-S, Lin Y-L, Zeng H-T, Chen C-Y and Liu C-L 2013 Orographic effects on heavy rainfall events over northeastern Taiwan during the northeasterly monsoon season; *Atmos. Res.* **122** 310–335, https://doi.org/10.1016/j.atmosres.2012.10.008.

Dimri A P 2004 Impact of horizontal model resolution and orography on the simulation of a western disturbance and its associated precipitation; *Meteorol. Appl.* **11** 115–127, https://doi.org/10.1017/S1350482704001227.

Edwards J M and Slingo A 1996 Studies with a flexible New radiation code. I: Choosing a configuration for a large-scale model; *Quart. J. Roy. Meteor. Soc.* **122** 689–719.

Gregory D and Rowntree P R 1990 A mass flux convection scheme with representation of cloud ensemble characteristics and stability-dependent closure; *Mon. Weather Rev.* **118** 1483–1506, https://doi.org/10.1175/1520-0493(1990)118<1483:AMFCSW>2.0.CO;2.

Henneberg O, Henneberger J and Lohmann U 2017 Formation and development of orographic mixed-phase clouds; *J. Atmos. Sci.* **74**(**11**) 3703–3724.

Hoffman R N and Kalnay E 1983 Lagged average forecasting, an alternative to Monte Carlo forecasting; *Tellus A* **35A** 100–118, https://doi.org/10.1111/j.1600-0870.1983.tb00189.x.

Houze R A Jr 2012 Orographic effects on precipitating clouds; *Rev. Geophys.* **50** RG1001, https://doi.org/10.1029/2011RG000365.

Jayakumar A, Sethunadh J, Rakhi R, Arulalan T, Mohandas S, Iyengar G R and Rajagopal E N 2017 Behavior of predicted convective clouds and precipitation in the high-resolution unified model over the Indian summer monsoon region; *Earth Space Sci.* **4** 303–313, https://doi.org/10.1002/2016EA000242.

Jiang Q 2003 Moist dynamics and orographic precipitation; *Tellus A* **55** 301–316, https://doi.org/10.1034/j.1600-0870.2003.00025.x.

Kitoh A 1997 Mountain uplift and surface temperature changes; *Geophys. Res. Lett.* **24**(**2**) 185–188, https://doi.org/10.1029/96GL03953.

Krishnamurti T N, Dubey S, Kumar V, Deepa R and Bhardwaj A 2017 Scale interaction during an extreme rain event over South-East India; *Quart. J. Roy. Meteor. Soc.* **143** 1442–1458, https://doi.org/10.1002/qj.3016.

Lott F 1999 Alleviation of stationary biases in a GCM through a mountain drag parameterization scheme and a simple representation of mountain lift forces; *Mon. Weather Rev.* **127** 788–801, https://doi.org/10.1175/1520-0493(1999)127<0788:AOSBIA>2.0.CO;2.

Nagalakshmi R and Prasanna K 2016 2015 flood assessment in Kanchipuram District of Tamilnadu using GIS; *Rasayan J. Chem.* **9** 798–805.

Narasimhan B, Murty Bhallamudi S, Mondal A, Ghosh S and Mujumdar P 2016 *Chennai floods 2015 – A rapid assessment*; Interdisciplinary Centre for Water Research, Indian Institute of Science, Bangalore, 49p.

Ning S, Song F, Udmale P, Jin J, Thapa B R and Ishidaira H 2017 Error analysis and evaluation of the latest GSMap and IMERG precipitation products over eastern China; *Adv. Meteorol.* **2017**(**11**) 1–16, https://doi.org/10.1155/2017/1803492.

Phadtare J 2018 Role of Eastern Ghats orography and cold pool in an extreme rainfall event over Chennai on 1 December 2015; *Mon. Weather Rev.* **146** 943–965, https://doi.org/10.1175/MWR-D-16-0473.1.

Rapp R 1997 Use of potential coefficient models for geoid undulation determinations using a spherical harmonic representation of the height anomaly/geoid undulation difference; *J. Geodesy* **71** 282–289, https://doi.org/10.1007/s001900050096.

Sato T 2013 Mechanism of orographic precipitation around the Meghalaya Plateau associated with intraseasonal oscillation and the diurnal cycle; *Mon. Weather Rev.* **141** 2451–2466, https://doi.org/10.1175/MWR-D-12-00321.1.

Sironi A, Tekin B, Rigamonti R, Lepetit V and Fua P 2015 Learning separable filters; *IEEE Pattern Anal.* **37**(**1**) 94–106, https://doi.org/10.1109/TPAMI.2014.2343229.

Smith S A, Vosper S B and Field P R 2015 Sensitivity of orographic precipitation enhancement to horizontal resolution in the operational Met office weather forecasts; *Met. Apps.* **22** 14–24, https://doi.org/10.1002/met.1352.

Trenberth K E, Dai A, Rasmussen R M and Parsons D B 2003 The changing character of precipitation; *Bull. Am. Meteor. Soc.* **84** 1205–1218, https://doi.org/10.1175/BAMS-84-9-1205.

Unnikrishnan C K, Gharai B, Mohandas S, Mamgain A, Rajagopal E N, Iyengar G R and Rao P V 2016 Recent changes on land use/land cover over Indian region and its impact on the weather prediction using unified model; *Atmos. Sci. Lett.* **17** 294–300, https://doi.org/10.1002/asl.658.

Van Oldenborgh G, Otto F L, Haustein K and Achuta Rao K 2016 The heavy precipitation event of December 2015 in Chennai, India; *Bull. Am. Meteor. Soc.* **97**(**12**) S87–S91, https://doi.org/10.1175/BAMS-D-16-0129.1.

Vogel H, Förstner J, Vogel B, Hanisch T, Mühr B, Schättler U and Schad T 2014 Time-lagged ensemble simulations of the dispersion of the Eyjafjallajökull plume over Europe with COSMO-ART; *Atmos. Chem. Phys.* **14** 7837–7845.

Walcek C J 1994 Cloud cover and Its relationship to relative humidity during a springtime midlatitude cyclone; *Mon. Weather Rev.* **122**(**6**) 1021–1035, https://doi.org/10.1175/1520-0493(1994)122<1021:CCAIRT>2.0.CO;2.

Walters D, Boutle I and Brooks M *et al.* 2017 The Met office unified model global atmosphere 6.0/6.1 and JULES global land 6.0/6.1 configurations; *Geo. Sci. Model Dev.* **10**(**4**) 1487–1520, https://doi.org/10.5194/gmd-10-1487-2017.

Webster S, Brown A R, Cameron D R and Jones C P 2003 Improvements to the representation of orography in the Met office unified model; *Quart. J. Roy. Meteor. Soc.* **129** 1989–2010, https://doi.org/10.1256/qj.02.133.

Wilson D R and Ballard S P 1999 Amicrophysically based precipitation scheme for the UK meteorological office unified model; *Quart. J. Roy. Meteor. Soc.* **125** 1607–1636, https://doi.org/10.1002/qj.49712555707.

Wilson D R, Bushell A C, Kerr-Munslow A M, Price J D and Morcrette C J 2008 PC2: A prognostic cloud fraction and condensation scheme. I: Scheme description; *Quart. J. Roy. Meteor. Soc.* **134** 2093–2107, https://doi.org/10.1002/qj.333.

Wood N, Staniforth A, White A, Allen T, Diamantakis M, Gross M, Melvin T, Smith C, Vosper S, Zerroukat M and Thuburn J 2014 An inherently mass-conserving semi-implicit semi-Lagrangian discretization of the deep-atmosphere global non-hydrostatic equations; *Quart. J. Roy. Meteor. Soc.* **140** 1505–1520, https://doi.org/10.1002/qj.2235.

Yadav S and Indu J 2016 Estimation of vertical accuracy of digital elevation models over complex terrains of Indian subcontinent; *Int. Geosci. Remote Sens.* 6036–6039, https://doi.org/10.1109/IGARSS.2016.7730577.

Yarrakula K, Deb D and Samanta B 2013 Comparative evaluation of Cartosat-1 and SRTM imageries for digital elevation modelling; *Geo-spatial Inf. Sci.* **16**(**2**) 75–82, https://doi.org/10.1080/10095020.2012.747645.

Corresponding editor: Subimal Ghosh